Article

Tracking “Invisible” Alkylchlorocarbenes by Their p Absorptions: Dynamics and Solvent Interactions

Robert A. Moss, Jingzhi Tian, Ronald R. Sauers, and Karsten Krogh-Jespersen

J. Am. Chem. Soc., **2007**, 129 (32), 10019-10028• DOI: 10.1021/ja071799i • Publication Date (Web): 21 July 2007

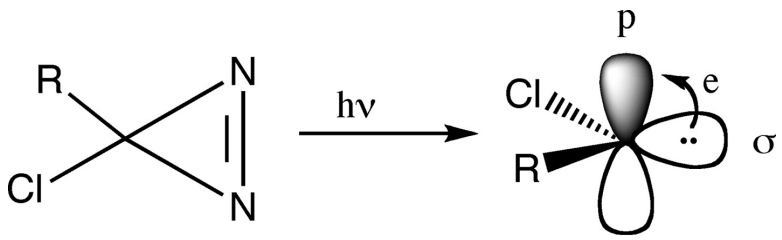

R = Me, $PhCH_2$, *t*-Bu, 1-Ad, or *c*-C_3H_5

More About This Article

Additional resources and features associated with this article are available within the HTML version:

- Supporting Information
- Links to the 5 articles that cite this article, as of the time of this article download
- Access to high resolution figures
- Links to articles and content related to this article
- Copyright permission to reproduce figures and/or text from this article

View the Full Text HTML

J|A|C|S
ARTICLES
Published on Web 07/21/2007

Tracking "Invisible" Alkylchlorocarbenes by Their $\sigma \rightarrow$ p Absorptions: Dynamics and Solvent Interactions

Robert A. Moss,* Jingzhi Tian, Ronald R. Sauers, and Karsten Krogh-Jespersen*

Contribution from the Department of Chemistry and Chemical Biology, Rutgers, The State University of New Jersey, New Brunswick, New Jersey 08903

Received March 26, 2007; E-mail: moss@rutchem.rutgers.edu; krogh@rutchem.rutgers.edu

Abstract: Contrary to implications in the literature, the $\sigma \rightarrow$ p absorptions of alkylchlorocarbenes (RCCl) are readily acquired by laser flash photolysis with UV−vis detection in solution at ambient temperature. Examples include RCCl with R = methyl, benzyl, *t*-butyl, 1-adamantyl, and cyclopropyl. These absorptions permit direct monitoring of carbene reactions and the formation of carbene−solvent complexes. The kinetics of the reactions of "free" and complexed MeCCl and $PhCH_2CCl$ were directly followed with tetramethylethylene and 1-hexene. Particularly effective complexation was provided by anisole and 1,3-dimethoxybenzene, which modulated the rates of intermolecular carbene additions. Computational studies are presented, which aid in understanding the carbene absorption spectra and the nature of the solvent complexes.

Phenylchlorocarbene (**1**) was the first singlet carbene whose intermolecular reactivity and associated fast kinetics were probed by laser flash photolysis (LFP) with UV detection.[1,2] Strong UV absorption at ∼310 nm, associated with the transition of an electron from a phenyl π orbital to the carbene's vacant p orbital, permitted efficient LFP-UV tracking of the carbene and enabled kinetics studies of its reactions with alkenes.[1,2]

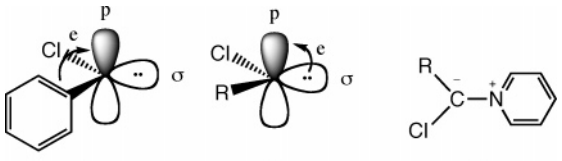

1 **2** **3**

a, R = Me; **b**, R = $PhCH_2$;
c, R = *t*-Bu; **d**, R = 1-Ad;
e, R = *c*-C_3H_5

Alkylchlorocarbenes (**2**, RCCl), which lack the $\pi \rightarrow$ p absorption, have been termed "invisible" carbenes.[3] Key examples of these species include methylchlorocarbene (**2a**), benzylchlorocarbene (**2b**), and *t*-butylchlorocarbene (**2c**).[3] It was tacitly assumed that the $\sigma \rightarrow$ p electronic transitions of **2** afforded absorptions that were simply too weak to be productively followed by LFP.

Accordingly, carbenes **2a**−**2c**, and RCCl in general, are usually visualized via their readily formed chromophoric pyridinium ylides (**3**), and the kinetics of their reactions are monitored indirectly by LFP.[3,4] We suspect that the simplicity of the pyridine ylide method discouraged attempts to observe the $\sigma \rightarrow$ p transitions of **2** in solution so that *direct* LFP studies of RCCl have gone largely unreported. Indeed, to our knowledge, the $\sigma \rightarrow$ p absorption of methylchlorocarbene, the parent alkylchlorocarbene, has never been documented.

Now we disclose that the $\sigma \rightarrow$ p absorptions of carbenes **2a**−**2e**, though weak, are readily observable in solution at ambient temperature by LFP, making it possible to directly monitor the kinetics of their intra- and intermolecular reactions.[5] More importantly, we can spectroscopically elucidate the interactions of RCCl with such solvents as anisole and 1,3-dimethoxybenzene, phenomena that cannot be readily probed by focusing on pyridine ylides **3**.

Results and Discussion

Methylchlorocarbene. LFP at 351 nm of 1.06×10^{-2} M methylchlorodiazirine[6,7] **4a** in pentane affords the spectrum shown in Figure 1a, recorded 50 ns after the laser pulse.[8]

We assign the principal absorption at 544 nm to the $\sigma \rightarrow$ p transition of MeCCl (**2a**) on the basis of several arguments. First, the observed signal agrees well with the calculated lowest

(1) Turro, N. J.; Butcher, J. A.; Moss, R. A.; Guo, W.; Munjal, R. C.; Fedorynski, M. *J. Am. Chem. Soc.* **1980**, *102*, 7576.
(2) Review: Moss, R. A.; Turro, N. J. In *Kinetics and Spectroscopy of Carbenes and Biradicals*; Platz, M. S., Ed.; Plenum Press: New York, 1990; pp 213 f.
(3) Jackson, J. E.; Soundararajan, N.; Platz, M. S.; Liu, M. T. H. *J. Am. Chem. Soc.* **1988**, *110*, 5595.
(4) (a) Jackson, J. E.; Platz, M. S. *In Advances in Carbene Chemistry*; Brinker, U. H., Ed.; JAI Press: Greenwich, CT, 1994; Vol. 1, pp 89 f. (b) Merrer, D. C.; Moss, R. A. *In Advances in Carbene Chemistry*; Brinker, U. H., Ed.; Elsevier: Amsterdam, 2001; Vol. 3, pp 53 f.
(5) Preliminary results were presented at the 18th IUPAC International Conference on Reactive Intermediates, Warsaw, Poland, August 23, 2006, and are contained in a written version of that talk: Moss, R. A.; Tian, J.; Chu, G.; Sauers, R. R.; Krogh-Jespersen, K. *Pure Appl. Chem.* **2007**, *79*, 993. Neither the spectra themselves, nor descriptions of the time-dependent dynamics of the carbene−solvent and carbene−diazirine reactions, are contained in this report.
(6) Graham, W. H. *J. Am. Chem. Soc.* **1965**, *87*, 4396.
(7) The extinction coefficient (69.6) of diazirine **4a** was determined from a linear correlation of *A* at 358 nm vs the concentration of **4a** from 0−0.02 M as determined by ^{1}H NMR vs an internal dioxane standard.
(8) Details of our LFP apparatus appear in the Supporting Information.

10.1021/ja071799i CCC: $37.00

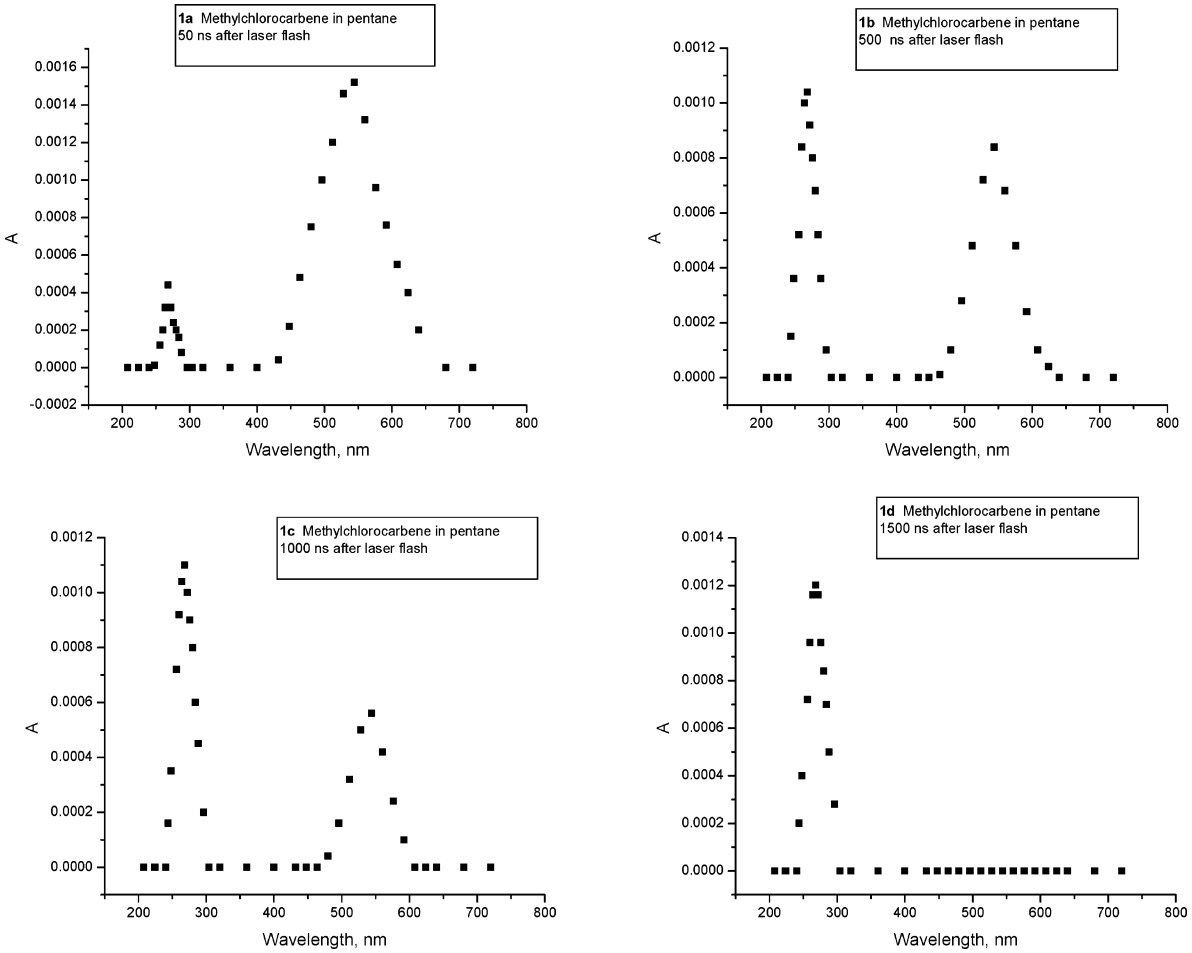

Figure 1. UV spectra of methylchlorocarbene in pentane generated by LFP (70 mJ) of diazirine **4a**: (a) 50 ns after laser pulse; (b) 500 ns after laser pulse; (c) 1000 ns after laser pulse; (d) 1500 ns after laser pulse. The diazirine concentration is 0.0106 M.

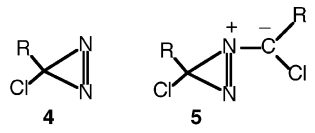

4 **5**

a, R = Me; **b**, R = $PhCH_2$;
c, R = *t*-Bu; **d**, R = 1-Ad;
e, R = *c*-C_3H_5

energy absorption of **2a**, computed at 556 nm in simulated heptane ($f = 0.005$) by TD-B3LYP/6-311+G(d) excited-state calculations at the PBEPBE/6-311+G(d) optimized geometry.[9] Examination of the transition amplitudes verifies that the elementary HOMO → LUMO excitation contributes highly (80%) to this transition. The HOMO of **2a** is the carbene lone pair orbital (>95% C σ-character), whereas the formally empty p orbital on the carbene center dominates the LUMO (86% C(2p) character, 14% Cl(3p) character). It thus appears appropriate to label this electronic transition and, by extension, analogous transitions in other alkylchlorocarbenes as $\sigma \rightarrow$ p. The intensity is weak because only the component of the electric dipole transition moment which is perpendicular to the C(Me)−C−Cl plane differs from zero (assuming effective C_s symmetry for **2a**). A rough experimental estimate of the extinction coefficient may be made by assuming that LFP of diazirine **4a** leads to $\sim 10^{-5}$ M of MeCCl. Given an absorbance of ~0.0016 for the carbene at 544 nm (Figure 1, top left) leads to an extinction coefficient of ~160.

The second lowest transition of MeCCl, a weak Cl(n) → p transition, is computed at much higher energy ($\lambda = 245.7$ nm, $f \sim 0.004$). This weak absorbance is not detected experimentally. There is literature precedent for the assignment of the long-wavelength absorption of MeCCl to a $\sigma \rightarrow$ p transition. Thus, Pliego et al. have carefully analyzed the electronic spectrum of PhCCl, demonstrating that the analogous long-wavelength absorption in this case also consists predominantly (86%) of electron promotion from the σ to p carbenic orbitals.[10]

Direct analysis of the first-order decay of the 544 nm absorption gives $k_{obs} = 2.0 \times 10^6$ s^{-1}, which mainly (but not completely, see below) reflects the 1,2-H shift of MeCCl to vinyl chloride and is in good agreement with $k_H = 1.4-3.0 \times 10^6$ s^{-1} for this reaction as determined by the pyridine ylide method.[11a,b] Further, a linear correlation of the rate constants for the decay of MeCCl at 544 nm as a function of the concentration of an added tetramethylethylene (TME) trap gives $k_{add} = 1.8 \times 10^9$ M^{-1} s^{-1} for the addition of MeCCl to TME; cf., Figure 2. This value is in reasonable agreement with $k_{add} = 1.3 \times 10^9$ M^{-1} s^{-1} determined (indirectly) using the pyridine

(9) See the Supporting Information for references to and details of the calculations.

(10) Pliego, J. R., Jr.; De Almeida, W. B.; Celebi, C., Zhu, Z.; Platz, M. S. *J. Phys. Chem. A* **1999**, *103*, 7481; cf., p 7484.

(11) (a) Bonneau, R.; Liu, M. T. H.; Rayez, M. T. *J. Am. Chem. Soc.* **1989**, *111*, 5973. (b) Dix, E. J.; Herman, M. S.; Goodman, J. L. *J. Am. Chem. Soc.* **1993**, *125*, 10424. (c) Liu, M. T. H.; Bonneau, R. *J. Am. Chem. Soc.* **1989**, *111*, 6873.

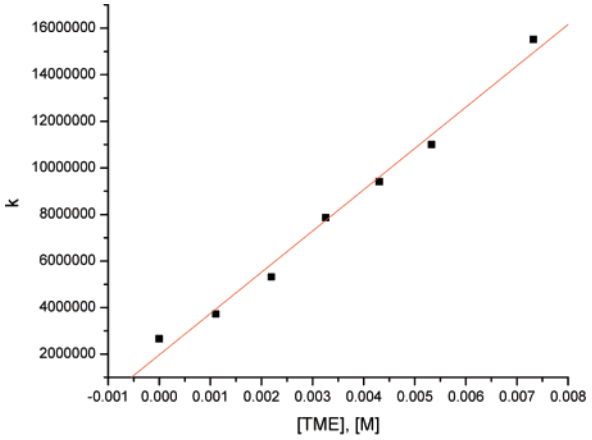

Figure 2. Observed rate constants (s^{-1}) for the quenching of MeCCl by TME in pentane, determined at 544 nm; slope = 1.77×10^9 M^{-1} s^{-1}, *Y*-intercept = 1.97×10^6 s^{-1}, $r = 0.994$.

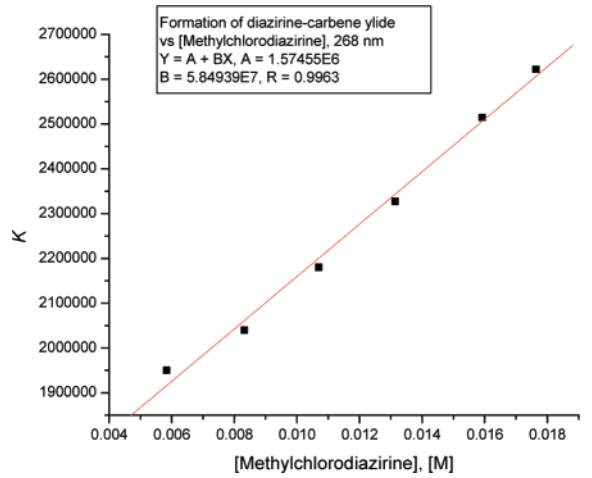

Figure 3. Observed rate constants (s^{-1}) for the formation of ylide **5a** vs [**4a**] (M), monitored at 268 nm.

ylide method.[11c] The *Y*-intercept of the correlation line in Figure 2, 2.0×10^6 s^{-1}, can also be taken as mainly reporting the hydride shift that converts MeCCl to vinyl chloride in the absence of TME. The intercept value is experimentally identical to the directly measured decay of MeCCl at 544 nm (see above).

Returning to Figure 1a, we assign the minor absorption at 268 nm to carbene−diazirine ylide **5a**, formed by reaction of MeCCl with diazirine **4a**; analogous ylides are reported to absorb at similar wavelengths.[12] In support of this assignment, a correlation of k_{obs} for the formation of **5a** as a function of diazirine concentration[7] is linear; cf., Figure 3. The slope, 5.8×10^7 M^{-1} s^{-1}, is the second-order rate constant for the reaction of MeCCl with **4a**, whereas the *Y*-intercept at [**4a**] = 0 gives the "corrected" first-order rate constant for the conversion of MeCCl to vinyl chloride by 1,2-hydride shift (k_H). This value, 1.6×10^6 s^{-1}, is ~25% less than "k_H" measured directly from the decay of MeCCl at 544 nm, because the latter includes a contribution from the competitive trapping of the carbene by **4a**.

An independent check on this conclusion is available from Figure 4, a correlation of k_{obs} for the decay of MeCCl at 544

(12) Bonneau, R.; Liu, M. T. H. *J. Phys. Chem. A* **2000**, *104*, 4115.

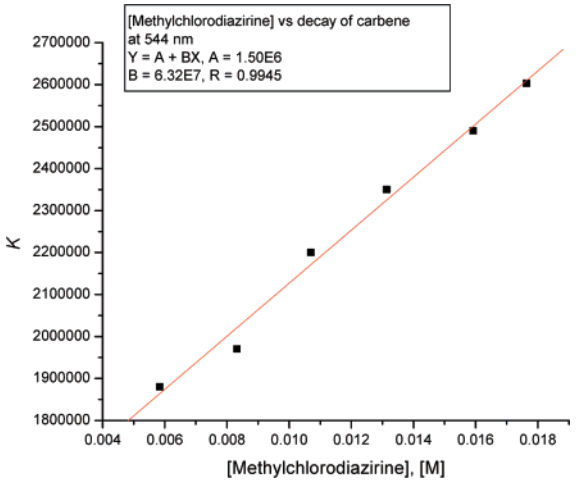

Figure 4. Observed rate constants (s^{-1}) for the decay of MeCCl at 544 nm vs [**4a**] (M).

nm with diazirine concentration. The slope (6.3×10^7 M^{-1} s^{-1}) and *Y*-intercept (1.5×10^6 s^{-1}) are in excellent agreement with those obtained from Figure 3 for the rate constants for ylide formation and hydride shift, respectively.

Finally, calculations predict the formation of ylide **5a** from reaction of MeCCl and **4a** to be very favorable ($\Delta G = -51.3$ kcal/mol, PBEPBE/6-311+G(d)). Furthermore, an intense $\pi-\pi^*$ type transition localized in the ylidic C−N−N triad is predicted to occur at $\lambda = 264.2$ nm ($f \sim 0.13$; TD-B3LYP/6-311+G(d) in simulated heptane solvent), in excellent agreement with the experimentally observed band at 268 nm.

Figure 1a−d furnishes a set of "snapshots" illustrating the evolution of MeCCl 50, 500, 1000, and 1500 ns after its generation from diazirine **4a** by LFP in pentane. We observe both the decay of MeCCl at 544 nm and the buildup of ylide **5a** at 268 nm.[13] After 1500 ns, only the absorption of ylide **5a** remains.

Solvent Interactions. Our newfound ability to track MeCCl by its $\sigma \rightarrow$ p absorption enables us to directly monitor carbene−solvent interactions, an important general problem in carbene chemistry which is difficult to resolve by indirect monitoring of carbene−pyridine ylides. For example, attempts to investigate interactions between phenylchlorocarbene, phenylbromocarbene, or *p*-nitrophenylchlorocarbene with, e.g., THF or MeCN, by LFP-UV tracking of the rates of carbene addition to TME, monitored via the carbene−pyridine ylides, were not definitive and could not detect possible weakly bound carbene−solvent complexes.[14] Similar difficulties attended a search for dichlorocarbene−ether interactions.[15] Better results were obtained when carbene−solvent interactions were followed by LFP with time-resolved IR monitoring,[16] but it seems clear that LFP-UV detection of carbene−solvent complexes will be optimized by direct observation of the carbene, rather than a derived ylide.

(13) The decay of ylide **5a** should provide an azine [MeClC═N−N═CClMe]. This product (in addition to vinyl chloride) was detected by GC−MS after 350 nm photolysis of diazirine **4a** in pentane. We have not kinetically monitored the decay of ylide **5a**.

(14) Celebi, S.; Tsao, M.-L.; Platz, M. S. *J. Phys. Chem. A* **2001**, *105*, 1158.

(15) Preslowski, S. I.; Zorba, A.; Thamattoor, D. M.; Tippmann, E. M.; Platz, M. S. *Tetrahedron Lett.* **2004**, *45*, 485.

(16) (a) Tsao, M.-L.; Zhu, Z.; Platz, M. S. *J. Phys. Chem. A* **2001**, *105*, 8413. (b) Sun, Y.; Tippmann, E. M.; Platz, M. S. *Org. Lett.* **2003**, *5*, 1305. (c) Tippmann, E. M.; Platz, M. S.; Svir, I. B.; Klymenko, O. V. *J. Am. Chem. Soc.* **2004**, *126*, 5750.

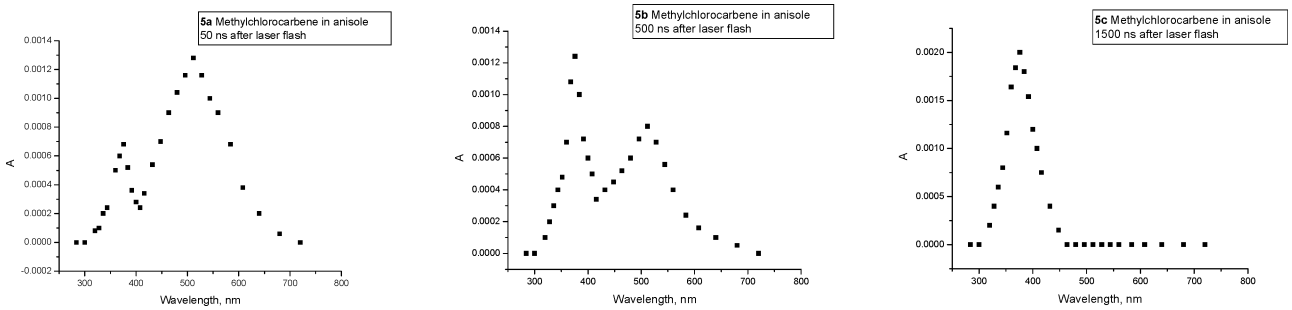

Figure 5. LFP-UV−vis spectra of MeCCl from diazirine **4a** in anisole: (a) 50 ns after the laser pulse; (b) 500 ns after the laser pulse; (c) 1500 ns after the laser pulse. The diazirine concentration is 0.0106 M, and the laser power is 70 mJ.

In this regard, we recall our previous calculations which suggested the formation of weak π and ylidic complexes between MeCCl and anisole.[17] Snapshots of the LFP-UV−vis spectra of MeCCl in anisole appear in Figure 5. There are three important differences between the MeCCl spectra in anisole and in pentane (cf., Figure 1). (1) Even at our shortest observation time (50 ns, Figure 5a), the MeCCl absorption at 544 nm in pentane has shifted to 520 nm in anisole. We consider this species to be an anisole-solvated carbene and calculate its $\sigma \rightarrow$ p absorption at 539 nm, $f = 0.005$, in simulated THF (representing anisole). (2) A new absorption appears at 368 nm in anisole. Over time, as illustrated in snapshots 5a−c, the solvated carbene absorption at 520 nm disappears in favor of the signal at 368 nm. Indeed, the latter absorption grows in with $k_{obs} = 3.7 \times 10^6$ s^{-1}, while the 520 nm absorption decays with the comparable rate constant, $k_{obs} = 3.2 \times 10^6$ s^{-1}. (3) In anisole, as opposed to pentane, there is no formation of carbene−diazirine ylide **5a**, viz. the absence of absorption below 300 nm. Presumably, MeCCl reacts with anisole solvent, bypassing reaction with the much less prevalent diazirine.

We attribute these spectroscopic phenomena, in particular observations (2) and (3), to the formation of weak MeCCl−anisole complexes, generically represented as **6**.[18] We have

MeC̈Cl/PhOMe
6

employed first-principles electronic structure techniques (MP2 and DFT with 6-311+G(d) basis sets) in an exhaustive search for such complexes. The DFT calculations have been carried out using both B3LYP and PBEPBE exchange-correlation functionals. Low binding energies of selected MeCCl/benzene and MeCCl/PhOMe complexes were obtained at the MP2/6-311+G(d,p)//MP2/6-31G(d) level in our prior study.[17] These complexes arose from weak electrostatic and dispersion forces. Traditionally, accurate representation of the weak, long-range electrostatic and dispersion interactions that hold such complexes together present difficulties for computational methods, even in small systems. We now find that DFT with the PBEPBE functionals produces a satisfactory compromise between accuracy and speed.[19] The complexation energies obtained with PBEPBE are qualitatively similar to those from MP2 calculations (see the Supporting Information), but they are typically 3−5 kcal/mol larger (less favorable). DFT calculations with the B3LYP functionals result in very small complexation energies (Supporting Information).

Regardless of the actual computational method applied, our searches reveal many weakly bound complexes corresponding to **6**; five representative structures are shown in Figure 6 as **6a**−**6e**.

Complexation energies, enthalpies, and free energies from PBEPBE/6-311+G(d) calculations (gas phase and simulated solvent) are summarized in Table 1; corresponding MP2 and B3LYP results (gas phase only) appear as Table S-1 in the Supporting Information.

Complexes **6a** and **6b** are of the π-type, where the key interaction involves electron donation from the aromatic π-system to the formally empty carbenic p orbital. The carbene center is located above an ortho C (**6a**) or a para C (**6b**) atom, and the carbene's Me group points toward the center of the phenyl ring, suggesting the presence of additional stabilizing C−H$\cdots\pi$-(aromatic) interactions.[20] Complex **6c** is both π-type and ylidic in nature. The carbene center is approximately equidistant to the ipso C and O atoms, and the Me group is oriented toward the center of the phenyl ring. Relative to **6c**, the ylidic $O^{\delta+}\cdots C^{\delta-}$ interaction is strengthened in **6d**, but the π-interaction has diminished. The O atom is approximately sp^3 hybridized in **6d** (the fourth site is occupied by a lone pair), and the Cl atom points toward the phenyl center.[21] Finally, in **6e** the carbene engages in primary H-bonding from its Me group to the anisole O atom. There is also secondary H-bonding interaction between an H atom of the anisole Me group and the empty carbenic p orbital. Trial geometries for a "meta π-complex" collapsed to para or ortho π-complexes upon energy minimization, in accord with the anisole methoxy group being strongly *o*, *p* electron donating.

As shown in Table 1, the computed binding energies of anisole complexes **6a**−**6e** (in the idealized gas phase and in simulated solvent) are small; complexation will be weak.

(17) Krogh-Jespersen, K.; Yan, S.; Moss, R. A. *J. Am. Chem. Soc.* **1999**, *121*, 6269.
(18) The LFP-UV spectrum of MeCCl in anisole is identical under air or nitrogen, excluding the intervention of a carbene−oxygen ylide (carbonyl oxide).
(19) We would expect the MP2 method to produce the more accurate interaction energies because dispersion interactions are included in this method. However, MP2 calculations scale poorly with molecular size and are cumbersome to use in exhaustive studies of potential energy surfaces for larger molecular systems. DFT, on the other hand, scales favorably with system size but does not generally include dispersion interactions in the functionals employed. That the PBEPBE functionals tend to err on the side of overbinding, whereas the B3LYP functionals underbind, particularly for weak interactions, probably works in our favor here.
(20) Nishio, M.; Hirota, M.; Umezawa, Y. *The CH−π Interaction: Evidence, Nature, and Consequences*; Wiley: New York, 1998.
(21) Attempts to reorient the carbene Me group of **6d** toward the phenyl center resulted (upon structural reoptimization) in rotation of the carbene back to its original position or in migration to complex **6c**.

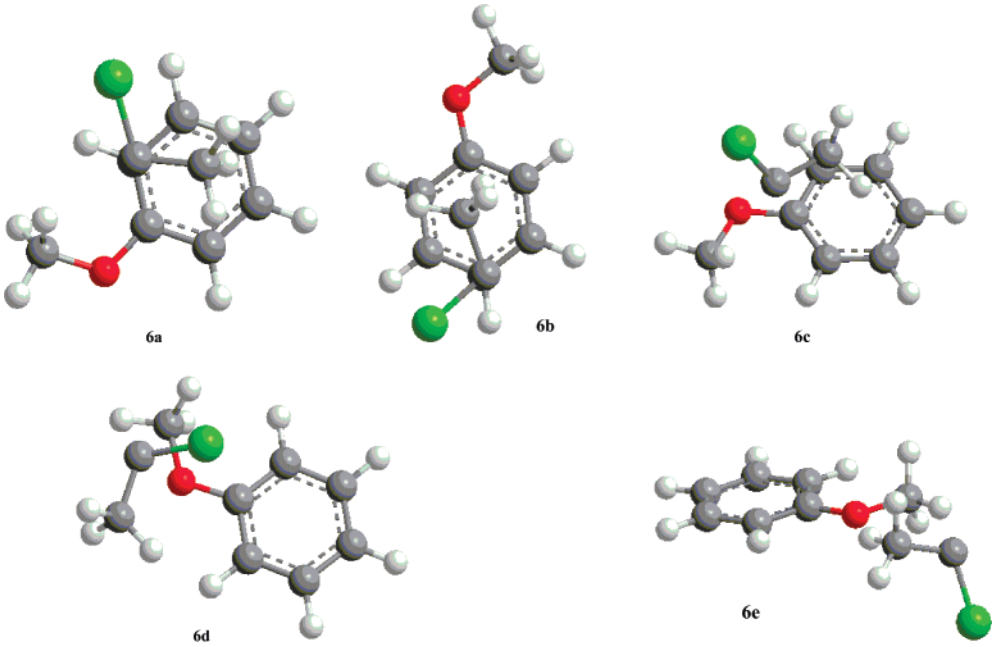

Figure 6. PBEPBE/6-311+G(d) computed structures of MeCCl/PhOMe complexes: **6a**, ortho π-complex; **6b**, para π-complex; **6c**, ipso π-complex; **6d**, ylidic complex; **6e**, H-bonded complex.

Table 1. Complexation Energies (PBEPBE/6-311+G(d)) for MeCCl + Solvent → 1:1 MeCCl/Solvent[a]

	gas phase			solution[d]		
complex	ΔE	ΔH^b	ΔG^c	ΔE	ΔH^b	ΔG^c
MeCCl/PhOMe, **6a**	−4.67	−3.35	5.13	−3.03	−1.88	5.73
MeCCl/PhOMe, **6b**	−2.81	−1.53	5.39	−3.15	−1.91	5.09
MeCCl/PhOMe, **6c**	−3.88	−2.64	3.89	−2.43	−1.91	5.74
MeCCl/PhOMe, **6d**	−3.18	−1.79	6.36	−2.47	−1.10	6.58
MeCCl/PhOMe, **6e**	−3.54	−2.35	4.01	−2.59	−1.98	5.99
MeCCl/benzene	−2.49	−1.29	5.12	−1.89	−0.73	5.70
MeCCl/THF	−7.40	−4.73	5.26	−9.44	7.26	4.72
MeCCl/dioxane	−5.59	−3.81	6.17	5.88	−3.70	7.26

[a] Energies are in kcal/mol, relative to the energies of separated reactants (one MeCCl plus one solvent molecule). [b] $T = 298.15$ K. [c] The free energy differences were computed using a reference state of 1 M concentration for each species participating in the reaction, and $T = 298.15$ K. [d] General solvent effects were incorporated via the CPCM model (see the Supporting Information).

Moreover, the Gibbs free energies of complexation are positive so that even in pure anisole the equilibrium between free and complexed MeCCl will favor the "free" carbene. The spread in complexation energies is 2−3 kcal/mol with no individual complex emerging as distinctly favored in either the "gas phase" or "solvent" calculations. An energy rank order of the structures **6a**−**6e** cannot be established on the basis of these computational results.[22]

Structures **6a**−**6e** in Figure 6 illustrate well-characterized minima on the potential energy surface, but additional minima surely exist. For example, **6a** represents the Me group located above the phenyl π-system, but there is an analogous species, which is also a minimum, where the Cl atom is above the phenyl π-system. A similar situation holds for **6b**, and the two ortho positions in anisole are in fact not fully equivalent so that slightly different "ortho" isomers exist as well. In the cases of **6a** and **6b**, the energy differences between such "rotamers" are of the order of 0.5−1.0 kcal/mol. Figuratively, the potential energy surface is pocketed with many shallow indentations ("craters") in horizontal planes ca. 3 Å above (or below) the anisole ring, where MeCCl/PhOMe complex formation may take place. In each crater, the carbene species enjoys considerable rotational freedom and presumably samples a wide swath of angular orientations. Importantly, we anticipate that a thermal equilibrium population is established among all of these binding sites.

Nevertheless, despite the small binding energies, sufficient complex is present in anisole to provide a spectroscopic signature at 368 nm, an absorption that is considerably more intense than the anisole-solvated carbene signal at 520 nm, and ultimately supplants it; cf., Figure 5. We find that the B3LYP functionals in conjunction with the PBEPBE optimized geometries provide a near optimal mix of computational conditions in TD-DFT calculations of **6**. Predicted electronic transition wavelengths and intensities (oscillator strengths, *f*) (TD-B3LYP/6-311+G(d)//PBEPBE/6-311+G(d)) appear in Table 2.

The calculations reveal three electronic transitions above 300 nm for complexes **6a**−**6e**. The two transitions of lower energy span wide spectral ranges because they represent spectroscopic signatures of the carbene−anisole interactions. The lowest energy transition, which spans an approximate range of $\lambda \sim 505-565$ nm, is the perturbed, but still well-localized, carbene σ → p excitation in the MeCCl−anisole complex. Due to the low concentration of complex, these transitions probably contribute to the broadness of the 520 nm band (Figure 5), but they do not form a distinct absorption band. The higher energy transition, which spans an approximate range of $\lambda \sim 380-445$ nm, is a π(anisole, HOMO) → p(carbene) charge-transfer transition. The computed intensity of this charge-transfer transition varies dramatically among the complexes, reflecting the magnitude of the overlap between the donor and acceptor orbitals, but the intensity is particularly large for two complexes: **6b** and **6d**. In these two complexes, the primary

(22) Consideration of the gas-phase MP2/6-311+G(d) and B3LYP/6-311+G(d) energies (Supporting Information) does not alter this conclusion.

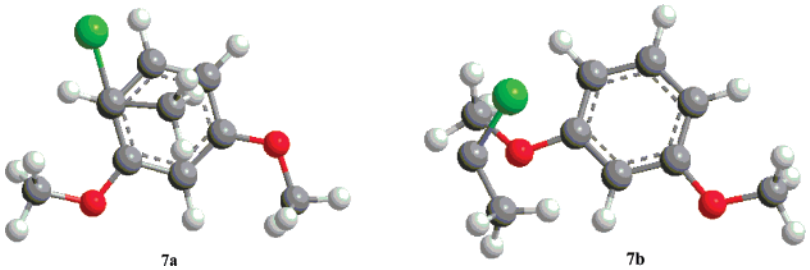

Figure 7. PBEPBE/6-311+G(d) computed structures of MeCCl/1,3-DMB complexes: **7a**, π- complex; **7b**, ylidic complex.

Table 2. Absorption Wavelengths and Oscillator Strengths (*f*) of 1:1 MeCCl/Solvent Complexes[a,b]

species	solvent [c]	λ_1	f_1	λ_2	f_2	λ_3	f_3	exp/solvent[d]
MeCCl	heptane	556.2	0.005	245.7	0.004	213.7	0.011	544/pentane
MeCCl	THF	538.7	0.005	246.1	0.004	211.3	0.008	520/anisole
MeCCl	benzene	554.8	0.005	245.9	0.004	213.4	0.011	544/benzene
MeCCl/PhOMe, **6a**	THF	564.0	0.023	417.5	0.034	330.6	0.078	
MeCCl/PhOMe, **6b**	THF	533.1	0.029	390.9	0.132	332.6	0.003	520,368/anisole
MeCCl/PhOMe, **6c**	THF	544.6	0.004	444.6	0.012	337.8	0.011	
MeCCl/PhOMe, **6d**	THF	506.5	0.017	380.0	0.087	310.8	0.002	520,368/anisole
MeCCl/PhOMe, **6e**	THF	535.7	0.008	426.0	0.002	326.3	0.0001	
MeCCl/benzene[e]	benzene	546.0	0.010	336.5	0.001	332.0	0.068	not observed
MeCCl/THF	THF	306.5	0.044	252.1	0.089	250.1	0.004	not observed
MeCCl/dioxane	THF	370.5	0.028	235.3	0.075	227.8	0.110	not observed

[a] TD-B3LYP/6-311+G(d)//PBEPBE/6-311+G(d) with simulated experimental conditions (CPCM solvation model). Gas-phase geometries were used. [b] Wavelengths in nm. [c] Solvent used for computational purposes. THF parameters were used to represent the experimental solvents anisole, THF, and dioxane. Heptane parameters were used to simulate pentane. [d] Solvent used in experiment. [e] MeCCl−benzene complex.

anisole−carbene interaction site matches the atoms where the π(anisole, HOMO) has its largest electron density: the oxygen and para carbon sites. The two complexes **6b** and **6d** also possess the highest energy charge-transfer transitions, and we believe they are the principal species responsible for the absorption observed at 368 nm (Figure 5). Even though **6b** and **6d** may not be the energetically most favored complexes (Table 1), all the anisole complexes are in thermodynamic equilibrium, and the **6b** and **6d** complexes "light up" preferentially (large *f*) to dominate the observed spectrum. The third transition tabulated is also a π(anisole) → p(carbene) charge-transfer transition, but it involves an anisole donor orbital which does not interact very directly with the carbene p orbital. Hence, its energy is not so variable among the complexes and its predicted intensity is generally low. Thus, these transitions likely contribute to the overall broadness of the band in Figure 5 but do not constitute a separate spectroscopic feature.

Table 1 also presents computational results for complexes of MeCCl with benzene, THF, and dioxane. The benzene complex is necessarily of the π-type, whereas the THF and dioxane complexes are *O*-ylides. A troublesome mystery is the absence of spectroscopic signatures for MeCCl/THF or MeCCl/dioxane ylidic complexes. Experimentally, the spectrum of MeCCl in pentane (λ_{max} at 544 nm) is unchanged in benzene, THF, or 1,4-dioxane down to 200−220 nm. The complexation energies presented in Table 1 indicate that these complexes should be comparable in stability to anisole complexes **6**.[23] Perhaps interaction with the anisole π-system is very important for complex formation. Also, given the many potential binding sites available to the carbene when anisole is the solvent, there should be more complexes formed in anisole than in THF or dioxane, even though the stability of any given complex may be similar to the *O*-ylides possible with THF and dioxane. Table 2 indicates that the MeCCl/THF or dioxane ylidic complexes should absorb at $\lambda \sim 230-250$ nm with good intensities. However, in keeping with their failure to perturb the spectrum of MeCCl, we note (see below) that THF and dioxane also exert smaller effects than anisole on the reactivity of MeCCl.

We also studied MeCCl in 1,3-dimethoxybenzene (DMB), with results similar to those obtained in anisole. There is a small additional blue shift of the MeCCl absorption in DMB to 512 nm (520 nm in anisole, 544 nm in pentane). Furthermore, a MeCCl/DMB complex grows in at 375 nm: snapshots of the LFP-UV spectra at 50, 500, and 1500 ns after the laser pulse appear in the Supporting Information (Figure S1), clearly demonstrating the decay of MeCCl at 512 nm in favor of the new species at 375 nm.

A computational study of the MeCCl/DMB complex affords results similar to those described above for MeCCl/PhOMe. Although our calculations of the MeCCl/DMB potential energy surface were less extensive, several local minima around the perimeter of the phenyl ring were easily located; ylide-type structures could be located as well. The binding energies for the MeCCl/DMB complexes (Table S-3 in the Supporting Information) are only slightly more favorable (∼1 kcal/mol) than those presented above for MeCCl/PhOMe. The energy differences between the various well-characterized structures are again so small that a thermal population distribution of complexes should be established in solution. We find that two complexes, shown in Figure 7 as **7a** and **7b**, are most likely responsible for the spectral feature observed at 375 nm in DMB. **7a** is a π-complex with the carbene positioned above C-4, a highly electron-rich carbon atom because it is para to one

(23) MP2 and B3LYP results (Supporting Information) indicate that the THF and dioxane ylides could be less favorable than anisole *O*-ylide **6d**; however, the relative destabilization is not large.

Table 3. Rate Constants for Additions of MeCCl to Alkenes[a]

solvent	k_{TME} (M^{-1} s^{-1})[b]	k_{hex} (M^{-1} s^{-1})[c]	τ (ns)[d]
pentane[e]	1.8×10^9	3.2×10^7	312
anisole[f]	4.4×10^8	7.1×10^6	306
1,4-dioxane[e]	7.6×10^8	2.1×10^7	113
THF[e]	1.0×10^9	2.6×10^7	49
1,2-DMB[f,g]	4.1×10^8	7.2×10^6	260
1,3-DMB[h,i]	4.6×10^7	2.3×10^6	637

[a] At 25 °C; errors in rate constants are ±10−15%. [b] Rate constants for additions to tetramethylethylene. [c] Rate constants for additions to 1-hexene. [d] Lifetime of MeCCl determined from the inverse of the *Y*-intercept of the correlation of k_{obs} for the disappearance of MeCCl vs [alkene]. [e] MeCCl monitored at 544 nm. [f] MeCCl monitored at 520 nm. [g] 1,2-Dimethoxybenzene. [h] MeCCl monitored at 512 nm. [i] 1,3-Dimethoxybenzene.

methoxy group and ortho to the other. Charge-transfer transitions are predicted (TD-B3LYP/6-311+G(d)//PBEPBE/6-311+G(d) in simulated THF) for **7a** at $\lambda = 391.2$ nm ($f = 0.11$) and $\lambda = 362.8$ nm ($f = 0.09$).[24] **7b** is an ylidic complex predicted to absorb at $\lambda = 377.8$ nm ($f = 0.05$) and at $\lambda = 357.3$ nm ($f = 0.06$).

Kinetics of MeCCl Additions to Alkenes. Given that MeCCl forms spectroscopically active complexes with anisole and DMB, does the complexation affect the carbene's reactivity? We used LFP to determine the absolute rate constants for MeCCl additions to TME and 1-hexene in several solvents; the results appear in Table 3.

In anisole, the absorptions at 520 nm (for MeCCl) and at 368 nm (for complex **6**) are both quenched by TME with comparable rate constants: 4.4×10^8 and 5.1×10^8 M^{-1} s^{-1}, respectively; cf., Figures S2 and S3 in the Supporting Information. We take this as k_{add} for the addition of MeCCl to TME in anisole; it represents about a 3.8-fold decrease relative to k_{add} in pentane. With the 1-hexene substrate, there is a corresponding 4.5-fold decrease.

Interestingly, dioxane and THF generate smaller rate diminutions than anisole: the decreases in dioxane (relative to pentane) are factors of 2.5 and 1.5 with TME and 1-hexene, respectively, whereas with THF the corresponding factors are only 1.8 and 1.2. Possibly, the diminished ability of dioxane and THF to modulate k_{add} for the additions of MeCCl to alkenes is related to the absence of spectroscopically detectable complexes of the carbene with these solvents. When such complexes are observed, as with anisole, greater diminutions in k_{add} are also seen.

Larger kinetic effects are induced by 1,3-DMB, where we observe k_{add} decreases by factors of 39 and 14 with TME and 1-hexene, relative to the analogous MeCCl additions in pentane. Note that enhanced kinetic modulation does not occur with 1,2-DMB, which is very similar to anisole in both spectroscopic and k_{add} effects.

The observed decreases in k_{add} evoked by anisole and 1,3-DMB could be a consequence of the reversible formation of MeCCl−solvent complexes. Alternatively, the retardations might reflect the kinetic advantage of a free carbene in pentane relative to a specifically solvated and encumbered carbene in anisole or 1,3-DMB. Analogous rate effects were observed for addition reactions of halocarbene amides to TME in dioxane and THF relative to noncoordinating Freon-113.[16c]

Another aspect of MeCCl reactivity included in Table 3 is the carbene's lifetime, which is mainly governed by the rate of its 1,2-H shift leading to vinyl chloride. Two effects of solvent need to be considered here: a coordinating solvent should stabilize MeCCl's singlet ground state and extend its lifetime, whereas a polar solvent will stabilize the polar transition state for the 1,2-H shift, accelerate this reaction, and decrease the carbene's lifetime.[25] One interpretation of the data in Table 3 is that a *balance* of these solvent effects controls the lifetime. Thus, dioxane and THF predominantly stabilize the transition state so that the MeCCl lifetime is shorter in these solvents than in pentane. Anisole and 1,2-DMB stabilize both the ground and transition states to comparable degrees, affording little change in τ, whereas 1,3-DMB preferentially stabilizes the ground state leading to a doubling of the lifetime relative to pentane.

Benzylchlorocarbene. Studies of benzylchlorocarbene (**2b**) are central to our understanding of alkylhalocarbenes. Issues involving the existence of carbene/alkene complexes, the occurrence of excited diazirine rearrangements, and the intervention of quantum mechanical tunneling have been addressed through this carbene.[4b,25b,26]

LFP of benzylchlorodiazirine **4b**[6,27,28] in pentane, at 50 ns after the laser pulse, reveals the σ → p absorption of $PhCH_2$-CCl at 576 nm, as well as a carbene−diazirine ylide (**5b**) band at 270−280 nm, superimposed with a second carbene absorption[27] at ∼304 nm; cf., Figure 8. An expansion of the 250−350 nm region (Supporting Information Figure S4) shows the asymmetry of the 270−325 nm composite absorption due to the overlap of the latter two signals.

Parallel to the spectroscopy of MeCCl (see above, Figure 1), LFP snapshots of $PhCH_2CCl$ at several intervals after the laser pulse demonstrate the decay of the carbene and the rise of the carbene−diazirine ylide; the process is complete within 1000 ns. The decay of **2b** monitored at 576 nm gives $k_{obs} = 3.0 \times 10^7$ s^{-1}, mainly reflecting the 1,2-H shift of $PhCH_2CCl$ to β-chlorostyrene, and in reasonable agreement with $k_H = 4.9-6.7 \times 10^7$ s^{-1} determined by the pyridine ylide method.[11a,27,29,30] These rate constants are not corrected for carbene loss due to carbene−diazirine ylide formation.

We also obtained $k_{add} = 4.1 \times 10^8$ M^{-1} s^{-1} for the addition of **2b** to TME (Supporting Information Figure S5), in good agreement with $k_{add} = 6.2 \times 10^8$ M^{-1} s^{-1}, previously reported.[27] Note that the *Y*-intercept of the correlation line in Figure S5 is 2.9×10^7 s^{-1}, which again represents an approximate k_H for the 1,2-H shift of carbene **2b** and is in excellent agreement with $k_{obs} = 3.0 \times 10^7$ s^{-1} determined directly from the decay of **2b** at 576 nm.

We are able to use the newly observed σ → p transition of $PhCH_2CCl$ to study its interactions with solvents. LFP of diazirine **4b** in anisole leads to the spectra of **2b** presented in Figure 9. The spectrum obtained 50 ns after the laser pulse

(24) The "local" σ → p MeCCl transition is computed at 574.3 nm ($f = 0.04$) in **7a** and at 498.6 nm ($f = 0.04$)in **7b**.

(25) (a) Sugiyama, M. H.; Celebi, S.; Platz, M. S. *J. Am. Chem. Soc.* **1992**, *114*, 966. (b) Merrer, D. C.; Moss, R. A.; Liu, M. T. H.; Banks, J. T.; Ingold, K. U. *J. Org. Chem.* **1998**, *63*, 3010.
(26) (a) Liu, M. T. H. *Acc. Chem. Res.* **1994**, *27*, 287. (b) Platz, M. S. In *Advances in Carbene Chemistry*; Brinker, U. H., Ed.; JAI Press: Stamford, CT, 1998; Vol. 2, pp 133 f.
(27) Liu, M. T. H.; Bonneau, R. *J. Am. Chem. Soc.* **1990**, *112*, 3915.
(28) The extinction coefficient of diazirine **4b** was determined as 45.4 from a linear correlation of *A* at 356 nm vs [**4b**] from 0−0.04 M. The concentration of **4b** was determined by ^1H NMR vs an internal dioxane standard.
(29) Jackson, J. E.; Soundararajan, N.; White, W.; Liu, M. T. H.; Bonneau, R.; Platz, M. S. *J. Am. Chem. Soc.*, **1989**, *111*, 6874.
(30) k_H can also be determined by monitoring the decay of **2b** at 310 nm (ref 27), but product β-chlorostyrene absorbs in the 290−300 nm region. Following the 576 nm σ → p absorption is simpler.

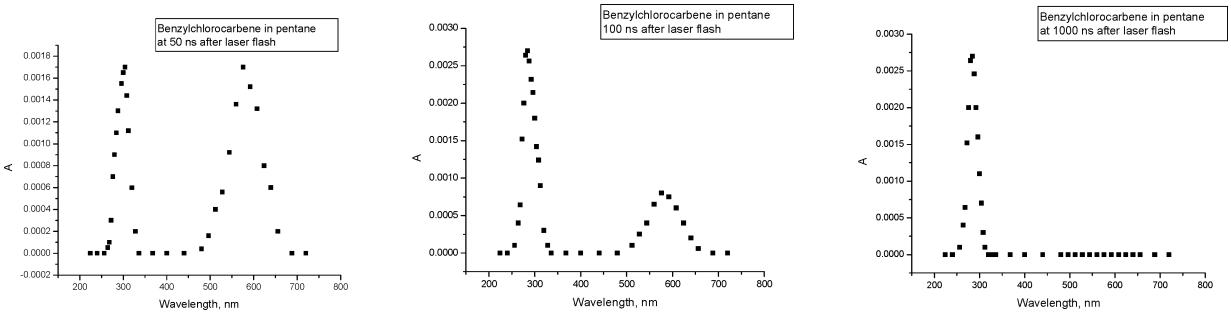

Figure 8. UV−vis spectra of benzylchlorocarbene in pentane generated by LFP (at 70 mJ) of 0.012 M diazirine **4b** at 50, 100, and 1000 ns after the laser pulse.

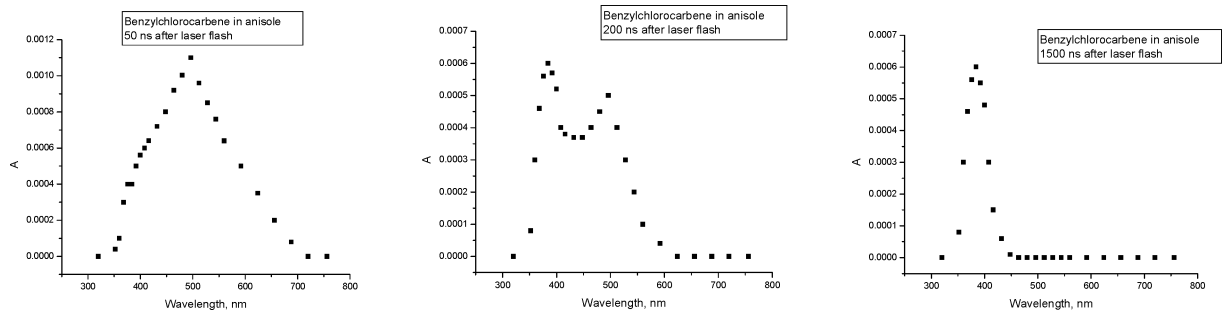

Figure 9. UV−vis spectra of carbene **2b** in anisole, generated by LFP of 0.012 M diazirine **4b**, at 50, 200, and 1500 ns after the 70 mJ laser pulse.

reveals that the $PhCH_2CCl$ absorption has moved from 576 nm (in pentane) to 496 nm in anisole, suggesting the formation of a **2b**−anisole complex represented generically as **8**. As time

$PhCH_2\ddot{C}Cl/PhOMe$
8

elapses, a shoulder visible at 370−390 nm grows into an absorbance at 380 nm (cf., the 200 ns snapshot in Figure 9). In analogy to our results with MeCCl, we assign the 380 nm signal to a **2b**−anisole complex. After 1500 ns, the carbene disappears in favor of the 380 nm species.

Analogous behavior attends the generation of $PhCH_2CCl$ in 1,3-DMB or 1,2-DMB. LFP snapshots of the 1,3-DMB experiments appear in Supporting Information Figure S6. Complexed carbene appears at 472 nm 50 ns after the laser pulse. Over time, this signal disappears in favor of a new species, presumably an ylidic variant of **8**, which grows in at 392 nm. After 1500 ns the process is complete, and only the latter species is seen. In 1,2-DMB, Supporting Information Figure S7 reveals three species 50 ns after the laser pulse: uncomplexed carbene at 572 nm, a $PhCH_2CCl$−1,2-DMB complex at 464 nm, and a probable ylidic complex represented by a shoulder at 376 nm. With time, the two longer wavelength species decay in favor of the 376 nm complex, which is the only survivor after 1500 ns.

Just as with MeCCl, the complexation of $PhCH_2CCl$ in anisole, 1,2-DMB, and 1,3-DMB has kinetic consequences for carbene additions to TME and 1-hexene. The results are collected in Table 4, where we find that, relative to pentane, anisole slows additions of $PhCH_2CCl$ to TME and 1-hexene by factors of 2.9 and 5.8, respectively. Somewhat larger decelerations of 3.7 and 11−14 are provided by 1,2-DMB, while 1,3-DMB evokes the largest retardations, factors of 18 (TME) and 31 (1-hexene). All three solvents provide ∼20-fold extensions of $PhCH_2CCl$ lifetime, from ∼30 ns in pentane to ∼600 ns. Anisole and (especially) 1,3-DMB appear to stabilize ground state $PhCH_2CCl$ by complexation and moderate its reactivity toward alkenes.

Table 4. Rate Constants for Additions of $PhCH_2CCl$ to Alkenes[a]

solvent	k_{TME} (M^{-1} s^{-1})[b]	k_{hex} (M^{-1} s^{-1})[c]	τ (ns)[d]
pentane[e]	4.1×10^8	6.9×10^7	33
anisole[f]	1.4×10^8	1.2×10^7	595
1,2-DMB	1.1×10^8 [g]	4.8×10^6 [g]	641[g]
	1.1×10^8 [h]	6.1×10^6 [h]	321[h]
1,3-DMB[i]	2.3×10^7	2.2×10^6	625

[a] At 25 °C; errors in rate constants are ±10−15%. [b] Rate constants for additions to tetramethylethylene. [c] Rate constants for additions to 1-hexene. [d] Lifetime of $PhCH_2CCl$ determined from the inverse of the *Y*-intercept of the correlation of k_{obs} for the disappearance of $PhCH_2CCl$ vs [alkene]. [e] $PhCH_2CCl$ monitored at 576 nm. [f] $PhCH_2CCl$ monitored at 496 nm. [g] $PhCH_2CCl$ monitored at 464 nm. [h] $PhCH_2CCl$ monitored at 572 nm. [i] $PhCH_2CCl$ monitored at 472 nm.

Other Carbenes. We include preliminary studies of three additional carbenes, which demonstrate that their $\sigma \rightarrow$ p absorptions can be readily acquired in solution by LFP. This will permit examination of their interactions with various solvents. LFP of *t*-butylchlorodiazirine **4c**[6,31] in pentane gave *t*-butylchlorocarbene **2c**, which displayed its $\sigma \rightarrow$ p absorbance at 544 nm; a carbene−diazirine ylide (**5c**) was also observed at 280 nm; cf., Supporting Information Figure S8.[32] The $\sigma \rightarrow$ p absorbance of **2c** was previously observed at 570 nm in a nitrogen matrix at 11 K.[33]

We followed the addition of *t*-BuCCl to TME via decay of the 544 nm absorption as a function of the alkene concentration

(31) Moss, R. A.; Munjal, R. C. *Chem. Commun.* **1978**, 775.
(32) This figure shows a "composite" of the carbene $\sigma \rightarrow$ p absorbance at 50 ns after the laser pulse and the carbene−diazirine ylide at greater elapsed time (1000 ns) so that the intensities of both signals are maximized.
(33) Zuev, P. S.; Sheridan, R. S. *J. Am. Chem. Soc.* **1994**, *116*, 4123.

in pentane. From a correlation of k_{obs} versus [TME] (Supporting Information Figure S9), we obtained $k_{add} = 3.0 \times 10^6$ M^{-1} s^{-1} and, from the *Y*-intercept at [TME] = 0, $k_{ins} = 3.3 \times 10^5$ s^{-1} for the 1,3-CH insertion of **2c** to 1,1-dimethyl-2-chlorocyclopropane. The latter value is not corrected for carbene−diazirine ylide formation but is in reasonable accord with $k_{ins} = 9.3 \times 10^5$ s^{-1} obtained by analysis of pyridine ylide data.[34] Note that the addition of *t*-BuCCl to TME in pentane is ∼600 times *slower* than the corresponding addition of MeCCl (see above). Presumably, the difference in reactivity is due to steric hindrance to addition originating at the *t*-butyl group of **2c**.

LFP of 1-adamantylchlorodiazirine **4d**[35] in pentane gave 1-adamantylchlorocarbene **2d** which displayed it σ → p absorbance at 545 nm, accompanied by carbene−diazirine ylide **5d** absorbing at 280 nm; cf., Supporting Information Figure S10.[32] The carbene signal has been observed at 540 nm in an argon matrix at 10 K[35] but not previously in solution. Correlation of k_{obs} for the decay of the 545 nm absorption as a function of the concentration of TME in pentane gave $k_{add} = 1.4 \times 10^7$ M^{-1} s^{-1} for the addition of **2d** to TME; cf., Supporting Information Figure S11. This is ∼5 times faster than the corresponding addition of *t*-BuCCl but ∼130 times slower than the addition of MeCCl to TME.[36]

The *Y*-intercept at [TME] = 0 of the correlation in Figure S11 gives $k = 4.0 \times 10^5$ s^{-1} for decay of the carbene in the absence of TME. Product studies reveal the decay product to be azine **9**, derived from reaction of **2d** with diazirine **4d**,

1-Ad-C(Cl)═N−N═C(Cl)-1-Ad
9

probably via intermediate ylide **5d**. Photolysis of carbene **2d** in an argon matrix gives chlorohomoadamantene by ring expansion,[35] but a thermal version of this reaction does not seem to compete with diazirine capture of **2d** in pentane solution at 25 °C.

LFP of cyclopropylchlorodiazirine **4e**[6] in pentane at 25 °C provided cyclopropylchlorocarbene, featuring a σ → p absorbance at 488 nm, a carbene−diazirine ylide (**5e**) absorbing at 270 nm, and a σ → σ_{C-Cl^*} carbene signal at 248 nm; cf., Supporting Information Figures S12 and S13.[37] The two carbene signals were previously observed in a nitrogen matrix at 14 K.[38] Decay of the 488 nm absorbance gave $k_c = 1.4 \times 10^6$ s^{-1} for the 1,2-C ring expansion of **2e** to 1-chlorocyclobutene, in reasonable agreement with $k_c = 9 \times 10^5$ s^{-1}, derived from decay of the 248 nm signal,[38] and 6×10^5 or 1.5×10^6 s^{-1} obtained by the pyridine ylide method.[10,38]

Conclusions. Contrary to implications in the literature,[3] the σ → p absorptions of alkylchlorocarbenes are readily acquired by LFP with UV−vis detection in solution at ambient temperature. Specific examples include RCCl where R = methyl, benzyl, *t*-butyl, 1-adamantyl, and cyclopropyl. The σ → p absorptions permit direct monitoring of carbene reactions and the formation of carbene−solvent complexes. The kinetics of the reactions of "free" carbenes and carbene complexes can be directly followed; examples of the latter are provided for MeCCl and $PhCH_2CCl$. Particularly effective complexation is provided by anisole and 1,3-DMB, which modulate the rates of intermolecular additions of MeCCl and $PhCH_2CCl$ to TME and 1-hexene. Computational studies aid in understanding the carbene absorption spectra and the nature of the carbene−solvent complexes.

Experimental Section

Diazirines. Diazirines **4a**−**4e** were prepared by Graham oxidation[6] of amidines, RC(═NH_2)NH_2•HCl. Acetamidine hydrochloride (R = Me) was purchased from Aldrich. Amidines with R = benzyl, *t*-butyl, 1-adamantyl, and cyclopropyl were prepared from the commercially available nitriles (RCN) by the Garigipati procedure.[39] The experimental procedure is described in detail for 1-adamantyl amidine hydrochloride in ref 39b, and the other amidines are cited in the literature.[40]

Methylchlorodiazirine (4a). Acetamidinium chloride (1.5 g) and 3 g of LiCl were added to 20 mL of DMSO in a 500 mL round-bottom flask, and the mixture was stirred magnetically for 20 min at 0 °C. Then, 200 mL of commercial bleach (12% by weight of aqueous NaOCl, saturated with NaCl, and cooled to 0 °C) was added with stirring over 30 min from an addition funnel. The reaction vessel was connected to a series of two traps; the first trap was cooled to −30 °C; the second trap was cooled to 77 K by liquid nitrogen. The reaction vessel was allowed to warm to ambient temperature as the system was evacuated to 1 mm of Hg for 30 min. Most of the diazirine **4a** condensed in the second trap. The vacuum was relieved; the diazirine was diluted with pentane or other solvent, and the diazirine solution was warmed to 0 °C. ***Caution.*** *Diazirines should be considered explosive, and preparative operations must be conducted behind shields.* Diazirine *solutions* seem to be safe.

^{1}H NMR (400 MHz, $CDCl_3$, δ): 1.66 (s, 3H). ^{13}C NMR (100 MHz, $CDCl_3$, δ): 24.58, 45.21. UV (pentane, nm): 325, 331, 348, 358 (max).

***t*-Butylchlorodiazirine (4c)** was prepared in the same manner except that methanol was substituted for the DMSO. ^{1}H NMR (400 MHz, $CDCl_3$, δ): 0.99 (s, 12 H). ^{13}C NMR (100 MHz, $CDCl_3$, δ): 27.03, 37.45, 50.89. UV (pentane, nm): 326, 332, 341, 348, 359 (max).

Cyclopropylchlorodiazirine (4e) was prepared in the same manner as **4a**. ^{1}H NMR (400 MHz, $CDCl_3$, δ): 0.41−0.42 (m, 2H), 0.64−0.66 (m, 2H), 1.58 (m, 1H). ^{13}C NMR (100 MHz, $CDCl_3$, δ): 5.13, 17.54, 25.89, 49.70. UV (pentane, nm): 340, 345, 355 (all equal, max), 377.

Benzylchlorodiazirine (4b). Benzylamidinium hydrochloride (2 g) and 4 g of LiCl were added to 40 mL of DMSO, and the mixture was stirred magnetically for 20 min at 0 °C. Then, 50 mL of pentane was added. Next, 300 mL of commercial bleach (12% by weight of aqueous NaOCl, saturated with NaCl, and cooled to 0 °C) was slowly added with stirring over 30 min. Stirring was continued for an additional 30 min at room temperature. Then, the pentane layer was separated and the aqueous phase was extracted twice with 50 mL portions of pentane. The combined pentane fractions were washed with 200 mL of ice water, dried over $MgSO_4$, and concentrated on the rotary evaporator to ∼5 mL. The residue was purified by chromatography over a short silica gel column, with pentane as the eluent, to give a pentane solution of **4b**.

^{1}H NMR (400 MHz, $CDCl_3$, δ): 3.33 (s, 2H); 7.27−7.29 (m, 2H), 7.37−7.41 (m, 3H). ^{13}C NMR (100 MHz, $CDCl_3$, δ): 43.74, 48.60, 127.91, 129.03, 129.76, 132.98. UV (pentane, nm): 341 (max), 349, 356.

(34) (a) Moss, R. A.; Ho, G.-J. *J. Am. Chem. Soc.* **1990**, *112*, 5642. (b) Moss, R. A.; Liu, W. *Chem. Commun.* **1993**, 1597.
(35) Yao, G.; Rempala, P.; Bashore, C.; Sheridan, R. S. *Tetrahedron Lett.* **1999**, *40*, 17.
(36) The steric substituent constants of *t*-butyl and 1-adamantyl are comparable: Hellmann, G.; Beckhaus, H.-D.; Rüchardt, C. *Chem. Ber.* **1979**, *112*, 1808.
(37) These spectra were acquired 50 ns after the laser pulse.
(38) Ho, G.-J.; Krogh-Jespersen, K.; Moss, R. A.; Shen, S.; Sheridan, R. S.; Subramanian, R. *J. Am. Chem. Soc.* **1989**, *111*, 6875.
(39) (a) Garigipati, R. S. *Tetrahedron Lett.* **1990**, *31*, 1969. (b) Moss, R. A.; Ma, W.; Merrer, D. C.; Xue, S. *Tetrahedron Lett.* **1995**, *36*, 8761.
(40) (a) R = $PhCH_2$: cf., ref 25b. (b) R = *t*-Bu: Moss, R. A.: Munjal, R. C. *Chem. Commun.* **1978**, 775. (c) R = *c*-C_3H_5: Moss, R. A.; Shen, S.; Krogh-Jespersen, K.; Potenza, J. A.; Schugar, H. J.; Munjal, R. C. *J. Am. Chem. Soc.* **1986**, *108*, 134.

1-Adamantylchlorodiazirine (4d) was prepared in the same manner as **4b** except that methanol replaced DMSO. ^{1}H NMR (400 MHz, $CDCl_3$, δ): 1.51 (d, J = 2.8 Hz, 6H), 1.57, 1.60, 1.65, 1.68 (3 AB systems, 6H), 1.99 (s, 3H). ^{13}C NMR (100 MHz, $CDCl_3$, δ): 28.23, 36.47, 38.55, 39.31, 56.22. UV (pentane, nm): 328, 334, 344, 350, 361 (max).

Azine 9. A solution of diazirine **4d** (A_{361} = 2.0) in 50 mL of pentane was irradiated at 350 nm in a Rayonet reactor for 2 h at 25 °C. The reaction mixture was concentrated to 10 mL and allowed to stand for 12 h. Colorless prisms of azine **9** precipitated, mp 190−191 °C. GC−MS (*m*/*e*): 392 (M^+), 357, 135. ^{1}H NMR (400 MHz, $CDCl_3$, δ): 1.70−1.77 (m, 12 H), 1.98−1.99 (m, 12H), 2.08 (s, 6H). ^{13}C NMR (100 MHz, $CDCl_3$, δ): 28.36, 36.67, 40.33, 43.40, 151.23.

LFP Studies. All LFP experiments were conducted at 25 °C on 2 mL of diazirine solutions in quartz cells. The diazirine absorptions were 0.8 at λ_{max} (see above). Carbene signals were monitored from 50 to 2000 ns after the laser pulse. Results with MeCCl and $PhCH_2CCl$ were identical under normal or nitrogen atmospheres. A description of the laser system appears in the Supporting Information.

Acknowledgment. We are grateful to the National Science Foundation for financial support. We thank Professor Robert Sheridan for helpful discussions.

Supporting Information Available: Description of the LFP installation, Figures S1−S13, details of the computational studies including optimized geometries and absolute energies for complexes **6a**−**6e** (PBEPBE/6-311+G(d)), complexation energies for **6a**−**6e** (MP2/6-311+G(d) and B3LYP/6-311+G(d)), electronic transition energies at the B3LYP/6-311+g(d) level for **6a**−**6e** at MP2/6-311+G(d) geometries, and complexation energies for **7** (PBEPBE/6-311+G(d)). This material is available free of charge via the Internet at http://pubs.acs.org.

JA071799I